

SPACE SCIENCES

Late accretionary history of Earth and Moon preserved in lunar impactites

Emily A. Worsham* and Thorsten Kleine

Late accretion describes the final addition of Earth's mass following Moon formation and includes a period of Late Heavy Bombardment (LHB), which occurred either as a short-lived cataclysm triggered by a late giant planet orbital instability or a declining bombardment during late accretion. Using genetically characteristic ruthenium and molybdenum isotope compositions of lunar impact–derived rocks, we show that the impactors during the LHB and the entire period of late accretion were the same type of bodies and that they originated in the terrestrial planet region. Because a cataclysmic LHB would have, in part, resulted in compositionally distinct projectiles, we conclude that the LHB reflects the tail end of accretion. This implies that the giant planet orbital instability occurred during the main phase of planet formation. Last, because of their inner solar system origin, late-accreted bodies cannot be the primary source of Earth's water.

INTRODUCTION

Late accretion describes the addition of material with a broadly chondritic bulk composition to planetary mantles after the cessation of core formation (1). On Earth, the late-accreted material is estimated to account for the final ~0.5% of Earth's mass and is thought to have been added after the Moon-forming giant impact, which likely induced the last major core formation event on Earth (1, 2). Hence, late accretion started immediately after formation of the Moon and is technically ongoing, albeit at a much-reduced rate. Determining the source and composition of late-accreted material is important not only for understanding the dynamics of the late stages of terrestrial planet growth but also because late accretion dominated by volatile-rich, carbonaceous chondrite-like material has been suggested to be the principal source of Earth's water and highly volatile elements (3, 4). However, it remains debated whether the late-accreted material derived from the inner or outer solar system and whether it was volatile rich (5–8).

Late accretion also includes a period called the Late Heavy Bombardment (LHB). As originally conceived, the LHB was proposed to account for the clustering of ^{40}Ar - ^{39}Ar , ^{87}Rb - ^{87}Sr , and U-Pb ages of Apollo lunar impact melt rocks between ~3.8 and ~4.0 billion years (Ga) ago (9, 10). It is important to recognize that the term LHB is not used consistently in the literature and is alternately used to refer to a "late" period of basin formation (i.e., after a stable crust formed) (11) or it is used synonymously with "lunar cataclysm," which refers to a sudden, short-lived surge in impact rate during which many of the large lunar impact basins were formed (10). Hence, the putative lunar cataclysm is only one possible mechanism by which the LHB may have occurred. Alternatively, the LHB may reflect the slowly declining bombardment during the accretion tail of terrestrial planet formation (12). In this case, the clustering of lunar impactites' ages may simply reflect a sampling bias by the dominance of ejecta from the ~3.9 Ga Imbrium Basin (13, 14). Consistent with this, some chronological studies have also found evidence for basin-forming impacts before the putative cataclysm, with ages inferred to represent the time of impact as old as ~4.3 to 4.2 Ga (15–17). Nevertheless, the

general agreement among the ^{40}Ar - ^{39}Ar age frequency distributions of Apollo samples, lunar meteorites, howardite-eucrite-diogenite meteorites (thought to derive from asteroid 4 Vesta), and H chondrites (18–20) indicates that an LHB occurred and affected the entire inner solar system (20, 21). Hence, there is no doubt that an LHB occurred, but its origin remains elusive (11, 22, 23).

A cataclysmic LHB would require a dynamic impetus that led to a sudden increase in impact rate. To account for this, it was proposed that a late migration of the giant planets scattered asteroids and comets into terrestrial planet-crossing orbits, resulting in a short-term, massive increase in the delivery of planetesimals into the terrestrial planet region ~600 million years (Myr) after their formation (the "Nice model") (24). However, more recent models suggest that the orbital instability of the giant planets, which is necessary to account for the orbital architecture of the outer solar system (25), occurred much earlier than required for a lunar cataclysm, during the first ~100 Myr of solar system formation (26–30). If correct, this would favor an accretion tail origin of the LHB because otherwise, there is no currently known dynamical process that may have triggered a late, cataclysmic bombardment of the Moon. Therefore, finding independent evidence for or against a cataclysmic LHB may provide additional insight into the time of the giant planet instability.

The cataclysmic and accretion tail origins of the LHB generally differ in the sources of the impactors involved. In an accretion tail scenario, the LHB impactors should derive from the same planetesimal population as those of the entire period of late accretion. By contrast, the impactor population resulting from a dynamically driven, cataclysmic LHB would be genetically distinct because it would, at least partially, derive from a destabilized planetesimal disk outside the terrestrial planet region (20, 24). Distinguishing between the two origins of the LHB may, therefore, be possible by determining the nebular source region(s) of the LHB impactors (i.e., terrestrial planet forming region, main asteroid belt, and/or outer solar system). Moreover, provided that the LHB impactors derive from the same population of bodies as the late-accreted material in general, determining their provenance may also allow determining the origin of the late-accreted material.

Previous studies have primarily used the relative abundances of highly siderophile elements (HSE) in lunar impactites to infer the composition and source(s) of lunar impactors (31–36). Owing to

Copyright © 2021
The Authors, some
rights reserved;
exclusive licensee
American Association
for the Advancement
of Science. No claim to
original U.S. Government
Works. Distributed
under a Creative
Commons Attribution
NonCommercial
License 4.0 (CC BY-NC).

Institut für Planetologie, University of Münster, Wilhelm-Klemm-Str. 10, Münster 48149, Germany.

*Corresponding author. Email: worsham@uni-muenster.de

their strong affinity to metal, the HSE were nearly quantitatively removed from the silicate portion of the Moon, and so, virtually all the HSE in lunar impactites derive from the projectiles. The HSE elemental and isotopic systematics in the impactites, therefore, reflect those of the impactor(s). Previous studies have shown that the relative HSE abundances of some bulk lunar impactites resemble those inferred for the bulk silicate Earth (BSE), suggesting that there may be a link between the late accretionary materials added to the lunar surface and the BSE (37). However, because of the large compositional range among the impactites and the potential for postimpact processes to affect HSE compositions [e.g., via fractionation during metal-sulfide-silicate segregation (36)], these data are more difficult to interpret in terms of the nebular source region(s) of the impactors. To this end, both an enstatite chondrite-like composition and inner solar system origin for the progenitor impactors (31) and a mixed impactor population including carbonaceous chondrites from the outer solar system have been proposed (36).

We use an approach that has previously not been applied to lunar impactites to determine the source(s) of lunar impactors, which relies on nucleosynthetic isotope anomalies in the siderophile elements Ru and Mo. Unlike trace element abundances or mass-dependent isotope fractionations, these nucleosynthetic anomalies are not expected to be affected by postimpact processes. Moreover, for both elements, nucleosynthetic isotope heterogeneity exists at the bulk meteorite and planetary scale and between the non-carbonaceous (NC) and carbonaceous (CC) meteorite reservoirs (38–43), which likely represent the inner and outer regions of the protoplanetary disk (44, 45), respectively. Together, this makes Ru and Mo isotope anomalies uniquely useful for discriminating material originating in different regions of the accretion disk and for identifying the nebular source reservoir(s) of LHB impactors.

Here, we report Ru and Mo isotope data for five chemically diverse lunar impactites (Fig. 1 and table S1), which we use to assess

whether the source of some of the impactors that struck the Moon during the LHB was similar to that of the population that impacted Earth and Moon during the entire period of late accretion. This comparison has important implications for the origin of the LHB, for the source and nature of late accretion in general, and for the prevailing dynamical environment of the time.

RESULTS

The samples of this study include three Apollo 16 impact melt rocks (60315, 62235, and 68815) and two feldspathic breccia meteorites [Northwest Africa (NWA) 11228 and NWA 5000]. The Apollo 16 samples have ^{40}Ar - ^{39}Ar ages of ~ 3.9 Ga at the supposed time of the lunar cataclysm (13, 46). Chronological information on the two lunar meteorites is sparse, but NWA 5000 may record an earlier impact event at ~ 4.1 to 4.2 Ga (47).

The Ru and Mo isotopic compositions of the lunar impactites are corrected for instrumental and natural mass-dependent fractionation and are reported in the ϵ -unit notation as the parts-in-10,000 deviations from terrestrial standard compositions. For determining the source of LHB impactors, we use $\epsilon^{100}\text{Ru}$ and $\epsilon^{102}\text{Ru}$ values because these are measured to the highest precision relative to other Ru isotope ratios, and $\epsilon^{94}\text{Mo}$ and $\epsilon^{95}\text{Mo}$ because the plot of $\epsilon^{94}\text{Mo}$ versus $\epsilon^{95}\text{Mo}$ best distinguishes NC and CC meteorites. We note, however, that all other isotope ratios are internally consistent for Ru and Mo, within uncertainty (see Materials and Methods). The lunar impactites have rather homogeneous Ru and Mo isotopic compositions, showing no resolved variations outside the analytical uncertainty of the measurements (Table 1 and tables S2 and S3). More specifically, the variance of the measurements is either comparable or slightly larger relative to the analytical reproducibility as estimated by repeated analyses of an iron meteorite, depending on the isotope ratio (i.e., the 2SD of $\epsilon^{100}\text{Ru}$ and $\epsilon^{102}\text{Ru}$ of the impactite measurements are ± 0.19 and ± 0.14 compared to the estimated reproducibility of ± 0.14 and ± 0.17 , respectively; the 2SD of $\epsilon^{94}\text{Mo}$ and $\epsilon^{95}\text{Mo}$ are ± 0.25 and ± 0.13 , compared to ± 0.18 and ± 0.14), indicating that there may be some small isotopic variations among the samples but which cannot currently be resolved. The observation that the samples measured here exhibit only slightly more variation than the analytical reproducibility of the measurements suggests that isotopic differences among individual impactors were either small or were homogenized by impact gardening (see discussion below) (48).

The new Ru and Mo isotopic data provide two first-order constraints on the nature and origin of the projectile material preserved in the investigated lunar impactites. First, the mean $\epsilon^{100}\text{Ru}$ of the impactites is -0.01 ± 0.12 [95% confidence interval (CI)], which is indistinguishable from the BSE. Thus, because the BSE's Ru almost entirely derives from late accretion (49), these data indicate that the Ru isotopic composition of the lunar impactites is indistinguishable from that of the late-accreted material in general (Fig. 2A). Second, in the $\epsilon^{94}\text{Mo}$ - $\epsilon^{95}\text{Mo}$ diagram, in which NC and CC meteorites lie along two distinct and approximately parallel lines, the impactites plot on the NC-line at $\epsilon^{94}\text{Mo} = 0.49 \pm 0.16$ and $\epsilon^{95}\text{Mo} = 0.20 \pm 0.08$ (95% CI; Fig. 2B), demonstrating that the projectiles sampled by the impactites of this study came from the inner solar system. Moreover, the combined Mo-Ru isotope systematics indicate that these projectiles on average had an enstatite chondrite-like isotopic composition (Fig. 3).

Below, we will first assess to what extent the lunar impactites of this study represent the population of bodies impacting the Moon

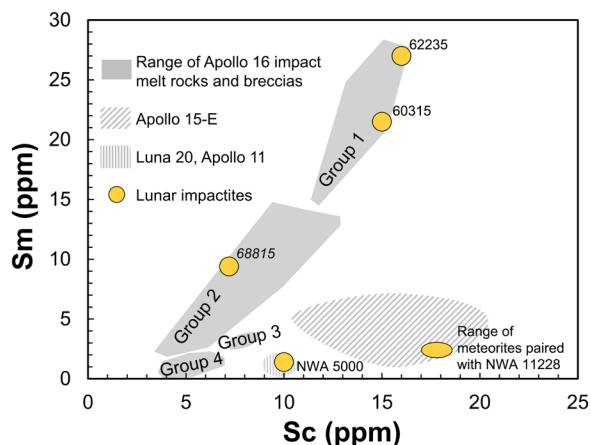


Fig. 1. Plot of Sc versus Sm concentrations for lunar impactites. Compositional fields are from (51). The Apollo 16 impactites studied here are shown relative to the full range of Apollo 16 impact melt rocks and breccias. The feldspathic breccia meteorites studied here plot outside the Apollo 16 compositional fields, suggesting that they sampled distinct target lithologies and are, therefore, from a different location on the Moon that is chemically similar to those sampled by some Apollo 15 and Apollo 11/Luna 20 impactites. Scandium and Sm data were not available for NWA 11228, so the range of Sc and Sm concentrations from meteorites that are likely paired with NWA 11228 (NWA 8673, 8746, 10065, and 11193) were used to represent NWA 11228 (70). Data references are in table S1.

Table 1. Ruthenium and Mo isotopic compositions of lunar impactites.

Sample, specific	Description	Age (Ga)*	N _{Ru} [†]	ε ¹⁰⁰ Ru	±	ε ¹⁰² Ru	±	N _{Mo}	ε ⁹⁴ Mo	±	ε ⁹⁵ Mo	±	Δ ⁹⁵ Mo‡	±
60315, 239	Poikilitic impact melt	3.868 ± 0.031	3	-0.12	0.14	-0.13	0.17	2	0.55	0.18	0.31	0.16	-2	19
62235, 303	Poikilitic impact melt	3.876 ± 0.032	2	-0.05	0.14	-0.02	0.17	5	0.59	0.14	0.16	0.08	-19	12
68815, 11	Glassy polymict breccia	3.6–4.1	2	-0.05	0.14	-0.05	0.17	5	0.28	0.17	0.18	0.11	1	15
NWA 11228	Feldspathic breccia		3	0.13	0.14	0.02	0.17	2	0.56	0.18	0.14	0.16	-19	19
NWA 5000	Feldspathic breccia	4.1–4.2	4	0.02	0.05	0.06	0.06	5	0.47	0.08	0.20	0.10	-8	11
Mean [§]				-0.01	0.12	-0.02	0.09		0.49	0.16	0.20	0.08	-9	12
Weighted mean [§]				0.01	0.08	0.03	0.08		0.49	0.12	0.19	0.05	-10	9
BSE*				0.00	0.02	0.00	0.02		0.04	0.06	0.10	0.04	7	5

*Ages for 60315 and 62235 from (46), 68815 from (13, 72), and NWA 5000 from (47). Ruthenium and Mo isotopic compositions of the BSE are from (7, 66). †N is the number of analyses of the same sample solution. Uncertainties for samples measured ≤3 times are the external reproducibility (2SD) determined by repeated analyses of an iron meteorite sample measured under the same conditions as the lunar samples. Uncertainties for samples measured >3 times are the 95% CI of the mean. ‡Δ⁹⁵Mo = (ε⁹⁵Mo - 0.596 × ε⁹⁴Mo) × 100 (66). Uncertainty is the propagated uncertainty on ε⁹⁴Mo and ε⁹⁵Mo. §Uncertainties are 95% CI of the mean. Weighted means were calculated using ISOPLOT (83) (see Materials and Methods).

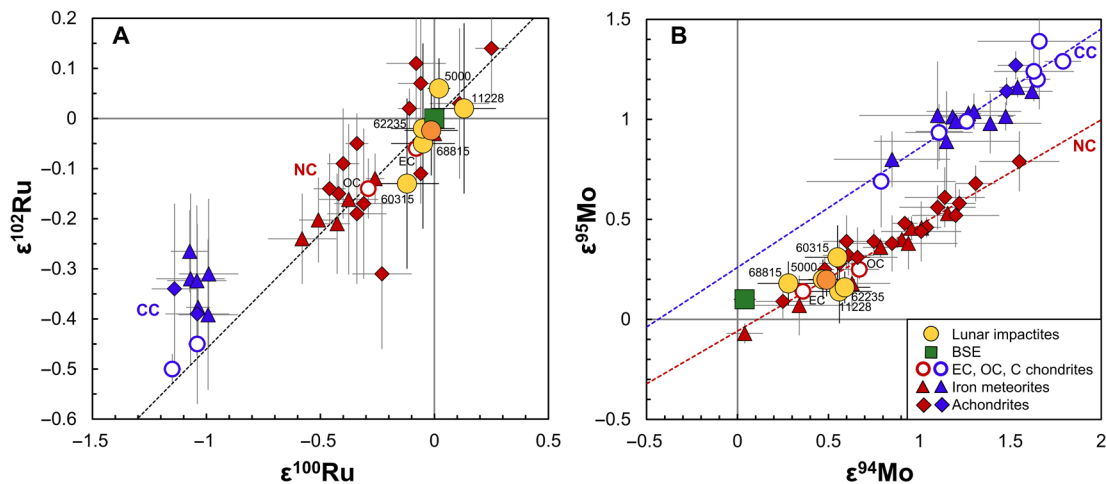


Fig. 2. Ruthenium and Mo isotopic compositions of lunar impactites. (A) ε¹⁰⁰Ru versus ε¹⁰²Ru and (B) ε⁹⁴Mo versus ε⁹⁵Mo. Data for individual lunar impactites (gold circles) and mean composition (orange circle) are plotted. The green square is the BSE isotopic composition (7, 66). Red and blue data points represent NC and CC meteorites, respectively, from (41, 82) and references therein. These data are also compiled in tables S7 and S8. (A) Dashed line is an s-process mixing line (84). (B) Red and blue dashed lines are the NC- and CC-lines defined in (66, 82). The average Ru isotopic composition of the lunar impactites is indistinguishable from the BSE, whereas in (B), the average Mo isotopic composition is resolved from the BSE and falls on the array defined by NC meteorites. Enstatite chondrites and aubrites have the most similar isotopic composition to the lunar impactites. Error bars for the lunar impactites are the 2SD of repeated analyses of an iron meteorite for samples with N ≤ 3 or the 95% CI of the mean for samples with N > 3.

during the LHB. We then discuss the origin of the LHB and the nature and provenance of late-accreted bodies in general.

DISCUSSION

Lunar impactites and the Moon’s impactor population

The five lunar impactites investigated here provide only a very limited spatial sampling of the lunar surface. Nevertheless, several lines

of evidence suggest that the isotopic composition of these impactites is the integrated signature of multiple impactors and, hence, provides information on the heritage of impactors for a sizable portion of the Moon. First, the samples derive from distinct areas of the Moon and, therefore, likely incorporated material from different impact basins. Second, even at a given location, multiple impactor signatures are present, indicating that the isotopic composition of each impactite likely represents the integrated signature of a few basin-forming

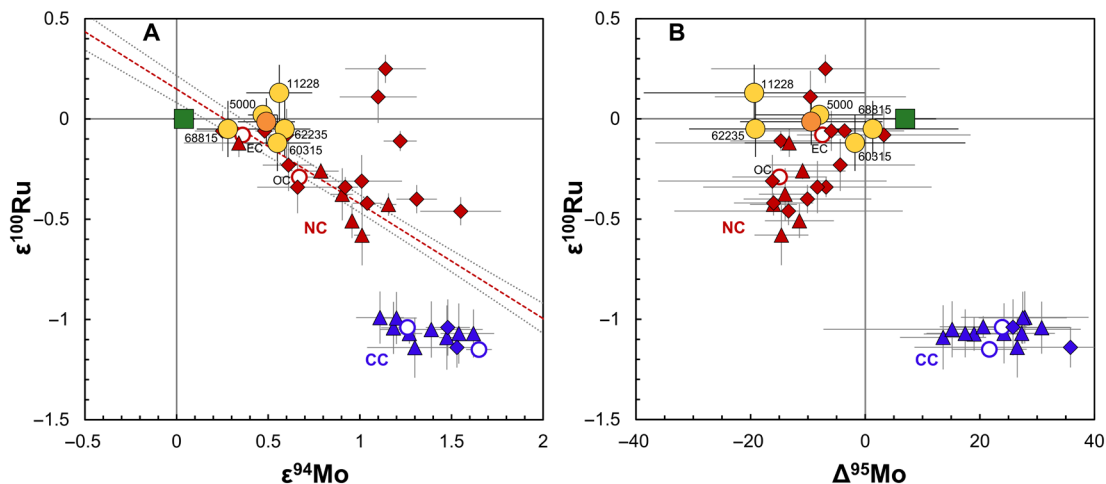


Fig. 3. Interelement Ru and Mo plots for the lunar impactites. (A) $\epsilon^{94}\text{Mo}$ versus $\epsilon^{100}\text{Ru}$ and (B) $\Delta^{95}\text{Mo}$ versus $\epsilon^{100}\text{Ru}$. $\Delta^{95}\text{Mo}$ is defined in Table 1. Data symbols and literature references are as in Fig. 2 and compiled in tables S7 and S8. (A) The lunar impactites fall on the Mo-Ru NC correlation defined in (41) and (B) among NC meteorites in $\Delta^{95}\text{Mo}$. The nonweighted means are plotted here. Error bars for the lunar impactites are the 2SD of repeated analyses of an iron meteorite for samples with $N \leq 3$ or the 95% CI of the mean for samples with $N > 3$. In (B), error bars on $\Delta^{95}\text{Mo}$ are the propagated $\epsilon^{94}\text{Mo}$ and $\epsilon^{95}\text{Mo}$ uncertainties.

impacts. Third, the average enstatite chondrite-like isotopic composition of the impactites is the same as the average composition of Earth's building material (50), which would be unexpected if the impactites recorded signatures of an unrepresentative population of impactors. Below, we will discuss this evidence in more detail.

First, on the basis of their mineralogy and major and trace element compositions, lunar impactites are subdivided into different groups, which represent distinct target rock precursors and/or parental impact melt sheets, or variable mixing proportions of clasts (51). Thus, impactites from different groups likely originated from distinct impacts or distinct areas within a single large impact melt sheet (and mixtures thereof). According to this classification, 60315 and 62235 belong to groups 1M and 1F, which means that they are both rather mafic, KREEP-bearing rocks (the K-REE-P-rich component is likely from the Procellarum KREEP terrane sampled by the Imbrium event). Both samples have some of the highest KREEP contents among Apollo 16 samples, indicating that they likely represent impact melt from the Imbrium basin. By contrast, sample 68815 falls into group 2, is more felsic than the other two Apollo 16 samples of this study, and has a lower KREEP contribution (52). Thus, although this sample, like 60315 and 62235, was collected from the Cayley Formation, 68815 likely samples a distinct impact melt and has a lower proportion of the Imbrium-related material (53). Last, the two NWA meteorites have lower REE and Th contents than the Apollo 16 impactites (54–57), indicating a lower KREEP content, and they have chemical similarities to the Apollo 15-E compositional group (NWA 11228) and some Luna 20 and Apollo 11 impact melts (NWA 5000) (51, 58, 59). This does not necessarily mean that these landing sites are the origin of these meteorites but does suggest that NWA 11228 and NWA 5000 originated from different areas of the Moon than the Apollo 16 samples (Fig. 1 and table S1).

Second, the HSE relative abundances of lunar impactites range from carbonaceous, ordinary, and enstatite chondrite-like to more fractionated compositions, similar to iron meteorites (31–36). This range of compositions suggests that these samples contain multiple impactor components, which occur in variable proportions among individual

impactites (36, 60). Specifically, whereas samples 60315, 62235, and 68815 have fractionated HSE abundances, similar to some iron meteorite groups (33, 60, 61), NWA 5000 has a relatively unfractionated HSE pattern, similar to enstatite chondrites (62), indicating that these samples represent chemically distinct impactor components. Despite these chemical differences, the Ru and Mo isotopic composition of the impactites measured here is indistinguishable within uncertainty. This suggests that either the impactors derive from an isotopically homogeneous reservoir or that isotopic heterogeneities were homogenized by spatial impact melt diffusion due to long-term impact gardening. The latter is consistent with numerical modeling of these processes (48), which suggests that the Apollo 16 landing site samples the Serenitatis and Nectaris impact melt (and, thus, the impactors) as well as the Imbrium impact melt. Similarly, although this is largely illustrative, if the NWA 5000 sample does originate from a similar region as the Luna 20 landing site, numerical modeling would suggest a fraction of Crisium, Smythii, and Nectaris impact melt in addition to Imbrium (48). The major basins likely redistributed material in a similar way as observed for Imbrium material today, and so, it is logical that large areas of the Moon contain a mixed signature of multiple basin-forming impactors. A corollary of this is that the homogeneous isotopic composition of the lunar impactites of this study provides a reasonable estimate for the average isotopic composition of impactors hitting the Moon.

Third, for all elements investigated so far, Earth is isotopically most similar to enstatite chondrites. This indicates that throughout accretion and including late accretion, Earth's major building blocks, on average, had the same enstatite-chondrite-like isotopic composition (50). This composition, however, is not well represented in the meteorite record, where most meteorites have more anomalous isotopic compositions relative to Earth. Hence, it would be unexpected that the impactites have the same isotopic composition as the majority of the building blocks of Earth if they only sample a limited number of impactors and are unrepresentative of the lunar impactor population. Moreover, that the three locations sampled on the Moon (from the meteorites and Apollo 16 samples of this study) all have an

enstatite chondrite-like composition would be unexpected, if not for the inferred large-scale mixing through impact gardening.

Together, the above considerations suggest that the two lunar meteorites probably derive from a different area of the Moon than the Apollo 16 samples (Fig. 1 and table S1), and all five impactites likely sample varying proportions of multiple basin-forming impactors. We, therefore, suggest that the Ru and Mo isotopic data of these samples combined provide a reasonable estimate for the composition of the impactors that struck a substantial portion of the Moon and, therefore, allow assessing the origin of the LHB. This hypothesis can be tested with future analyses of samples from other Apollo landing sites, which, owing to the lower Ru and Mo concentrations in these samples, will require the development of more sensitive analytical techniques or the consumption of larger sample masses than used here.

The LHB as the tail end of accretion

The Ru and Mo isotopic data of the lunar impactites can be used in two complementary ways to assess dynamical processes during the Moon's bombardment history and, specifically, whether the LHB was a cataclysmic event. First, the impactites' compositions may be compared to those of meteorites to establish the genetic relationship between projectiles hitting the Moon and a specific population of planetesimals as sampled by meteorites. Second, comparison of the lunar impactites' composition to that of the late-accreted material in general may be used to assess whether there was a change in the impactor population during the LHB. Combined, this may help to distinguish between a cataclysmic and accretion tail origin of the LHB, because whereas the former generally predicts a contribution of main belt asteroids and, potentially, comets to the LHB (24), the latter predicts a close link between LHB impactors and late-accreted materials.

A terminal lunar cataclysm, or any abrupt increase in the impact flux to the Moon, requires a dynamical event that destabilized the planetesimal disk and led to a sudden, short-term surge in the influx of impactors. For example, in the original Nice model, the migration of Jupiter and Saturn into a 1:2 orbital resonance destabilized the orbits of Neptune and Uranus (25) and scattered comets and asteroids from the primordial asteroid belt into the inner solar system, where they would have become potential impactors during the putative lunar cataclysm (24). Modified versions of the Nice model suggest that lunar impactors predominately originated from the primordial main asteroid belt (20) and/or the hypothetical extended (E) belt, which may have existed inward of the main asteroid belt and remnants of which may be the Hungaria asteroid group, consisting of mostly E-type asteroids (63, 64). Thus, depending on whether an orbital instability of the giant planets resulted in lunar impactors from the cometary disk (24), the primordial main asteroid belt (20, 24), and/or the E-belt (63, 64), it may have scattered isotopically distinct objects into the inner solar system. In the first case, we would expect the lunar impactites to have CC-like Mo and Ru isotope signatures with only little contribution from NC material, because the LHB impactors would be dominated by C-type (carbonaceous) asteroids and comets. In the second case, we would expect to see an isotopically anomalous, potentially mixed NC-CC signature in the lunar impactites, because the asteroid belt consists of a mixture of NC bodies with larger nucleosynthetic anomalies than Earth and CC bodies. Last, in the third case, we would expect the lunar impactites to have enstatite chondrite-like isotope signatures, because E-type asteroids are probably compositionally similar to aubrites and enstatite chondrites.

The lunar impactites of this study all have an NC-like Mo isotope composition (Fig. 2) and plot inside the NC field in the Mo-Ru isotope diagram (Fig. 3). Moreover, if NWA 5000 represents an earlier impact event (47) relative to the Apollo 16 samples, this would indicate that the dominant impactors were NC spanning the time of the putative lunar cataclysm. This does not exclude that individual impactors had a CC composition and, thus, is not inconsistent with the presence of carbonaceous chondrite-like HSE elemental and radiogenic Os isotope signatures identified in some lunar anorthositic regolith breccias (36), but does suggest that the impactors predominantly derive from the NC reservoir. This is inconsistent with the expected composition of LHB impactors in the aforementioned first two variants of the Nice model, which both predict considerable contributions of CC bodies and isotopically anomalous NC bodies to the LHB. Note that this conclusion holds even if the lunar impactites only sample the late stages of an instability-driven population dominated by asteroids (11), because the lunar impactites define an end-member composition compared to asteroids (as sampled by meteorites), so that a random mix of asteroids would not yield the isotopic composition observed for the impactites. Furthermore, the first two variants of the Nice model also predict that the LHB consisted of a different impactor population than late accretion in general, because the late orbital instability would have destabilized a planetesimal population that otherwise would not have contributed substantially to impacts onto the Moon. Thus, these variants of the Nice model are inconsistent with our finding that the LHB impactors derive from the same population of bodies as those accreted during the entire period of late accretion from ~4.4 to at least ~3.9 Ga ago. Consequently, provided that the lunar impactites studied here represent the projectiles that struck a large portion of the Moon during the LHB (see above), these data rule out that the LHB was caused by a late giant planet instability that resulted in lunar impactors predominately from either the cometary disk or the main asteroid belt.

By contrast, we cannot fully rule out the possibility that the impactites analyzed here predominately sampled E-belt asteroids, such as predicted in the third variant of the Nice model. In this case, there would still be a small contribution of main-belt asteroids to the cataclysmic LHB (e.g., two to three basins of ~12) (63, 64), and we would, therefore, expect an offset of the impactites' $\epsilon^{100}\text{Ru}$ toward more negative values (i.e., the typical values of main belt asteroids as sampled by meteorites). However, if anything, the $\epsilon^{100}\text{Ru}$ values of the lunar impactites are more positive than, albeit not resolved from, enstatite chondrites (Figs. 2 and 3). Thus, if future measurements on a larger sample set show similar compositions as observed here, it would preclude any appreciable contribution from main-belt asteroids and would, therefore, make a late instability less likely in general.

In contrast to a terminal cataclysm, a monotonically declining bombardment consisting of leftover planetesimals as the cause of the LHB would naturally result in identical Ru isotopic compositions of late-accreted materials and the lunar impactites. In this case, the impactors that contributed to late accretion and the LHB derive from the same population of planetesimals and, therefore, have the same isotopic composition. This model of the LHB does not require a specific late dynamical event that scattered planetesimals into the inner solar system, because the impactors that bombarded the terrestrial planets originated from orbits like those of the targets. This model also naturally accounts for the same, enstatite chondrite-like isotope composition of Earth's major building material, the

late-accreted material, and the lunar impactites, because all derive from the same population of bodies, which dominated the terrestrial planet region. Hence, we argue that an accretion tail origin of the LHB is the most straightforward and consistent interpretation of the isotopic data.

An accretion tail origin of the LHB implies that the required giant planet instability (25) occurred well before the LHB and before late accretion in general. Therefore, this interpretation is consistent with recent dynamical models that argue for an early giant planet orbital instability (26–30, 65). It also is consistent with the crater-size frequency distribution on the Moon, which has been interpreted to reflect a monotonically declining bombardment consisting predominantly of leftover planetesimals from the terrestrial planet region (12).

An NC late accretion

The Ru and Mo isotopic data for the impactites also have important implications for constraining the nature and provenance of late accretion in general. As a moderately siderophile element, the BSE's Mo predominantly derives from the final 10 to 15% of accretion (50), and so, its isotopic composition does not only record late accretion but also earlier-accreted material (66). By contrast, the BSE's Ru derives virtually entirely from late accretion, so the BSE's Ru isotopic composition is that of the average late-accreted material. The observation that the Ru isotopic composition of the lunar impactites is identical to that of the late-accreted material, therefore, implies that the Mo isotopic composition of the lunar impactites is also that of the average late-accreted material. This is important because the Ru isotopic composition of the BSE alone cannot unequivocally distinguish between an NC- and CC-dominated late accretion, because mixing with CC material would only change the Ru isotopic composition along the *s*-process mixing line (Fig. 2A). By contrast, Mo isotope systematics allow the NC and CC meteorites to be clearly distinguished (Fig. 2B). Consequently, that the lunar impactites plot on the NC-line in Mo isotope space close to enstatite chondrites (Figs. 2B and 3B) demonstrates that late-accreted material in general originated in the NC reservoir (i.e., the inner solar system) and, like the majority of Earth's building material (50), had an enstatite chondrite-like isotopic composition on average.

Our finding of an isotopically enstatite chondrite-like late accretion is consistent with earlier results based on the Os (2) and Ru isotope composition of the BSE (38) but contrast with the interpretations of some other recent studies. For instance, on the basis of the discovery of positive $\epsilon^{100}\text{Ru}$ in some Eoarchean terrestrial rocks, it was argued that late accretion also included material characterized by negative $\epsilon^{100}\text{Ru}$ and that this was carbonaceous chondrite-like material (7). Yet, most NC meteorites are also characterized by negative $\epsilon^{100}\text{Ru}$, and so the presence of material having negative $\epsilon^{100}\text{Ru}$ in the late accretionary assemblage does not require the incorporation of CC material. Previous studies also used Se-Te-S relative abundances (4) and mass-dependent Se isotope variations (8) to argue that late accretion consisted of volatile-rich carbonaceous chondrite-like material. However, these compositions may not be restricted to the CC reservoir, and they can be subject to fractionation processes in Earth's mantle, such that the BSE composition for these elements is not well constrained (67, 68). Hence, chemical- and mass-dependent isotope signatures of volatile elements such as Se, Te, and S provide less-stringent genetic tracers for the provenance of late accretion.

By contrast, the Mo isotopic composition inferred for late accretion from the lunar impactites is exclusive to the NC reservoir and,

if representative of late-accreted materials in general, would limit the mass fraction of CC material in the late accretion assemblage to less than ~20% (see Materials and Methods). Given that the estimated water and highly volatile element content of Earth may require the accretion of ~1 to 2% of Earth's mass of CI-like material (6), a late accretion of ~0.5% of Earth's mass with <20% CC contribution could not be a major source of Earth's volatiles. Hence, the NC-like Mo isotopic composition of the late-accreted material inferred from lunar impactites, along with the mixed NC-CC Mo isotopic compositions of the BSE (Fig. 2B) (66), implies that Earth accreted volatile-rich CC-like material before late accretion.

MATERIALS AND METHODS

Samples

The samples studied here were targeted for their relatively abundant metal, and they represent a range of compositions and textures (Fig. 1 and table S1). Apollo samples 60315 and 62235 are poikilitic impact melt rocks, whereas 68815 is a glassy polymict breccia consisting of various, generally small impact melt clasts in a glassy matrix (69). Northwest Africa 11228 consists of many millimeter- to centimeter-sized pieces and is described as a feldspathic fragmental breccia by the Meteoritical Bulletin. It is possibly paired with several other NWA meteorites, including NWA 8673 (70). Northwest Africa 5000 is a feldspathic breccia and contains gabbroic impact melt clasts in a dark impact melt matrix. The samples have a range of cosmic ray exposure (CRE) ages of 2.04 ± 0.09 Ma (68815), 5 ± 3 Ma (60315), 153 ± 3 Ma (62235), and ~600 Ma (NWA 5000) (71–73). Although prolonged CRE may modify Ru and Mo isotope compositions, this effect was evidently not important for the samples of this study because 68815 and NWA 5000 have indistinguishable Ru and Mo isotopic compositions despite their different CRE ages.

Because of the low abundance of Ru and Mo in the lunar crust (74, 75) and the comparatively high abundances in projectile materials, the Ru and Mo isotopic compositions of the impactites represent those of the impactors. The metals in the Apollo 16 samples have elevated average Ni contents, relative to endogenous metals formed via Fe reduction, ranging from ~5 (62235) to ~6.7 (60315) weight % (76, 77). This, in addition to the elevated HSE abundances in the Apollo 16 and meteorite metal, suggests an exogenous origin for these elements and likely most of the metal itself. An important question is whether impacts of oxidized, metal-poor material, like some carbonaceous chondrites, would result in impactites with little metal, such that sampling for this work could be biased to reduced, metal-rich impactors. However, the lunar target lithologies are reduced and would contain metal in the near surface from previous impacts, or minor native metal formed by Fe reduction. During the impact of an oxidized, metal-poor projectile, it is likely that the Ru and Mo would be scavenged into impact-remelted metal. Therefore, we suggest that sampling will not be appreciably biased in such a way.

Between ~3 and ~5 g of the Apollo samples and ~7 and ~19 g of the meteorites were powdered using an agate mortar and pestle dedicated for lunar samples only. The metal containing all the Ru and Mo was separated using a neodymium hand magnet from the progressively finer grain size fractions of the powder, yielding between 30 and 75 mg of metal and sulfides mixed with adhering silicate (table S4). Every effort was made to extract the total magnetic fraction, but it is likely that very small grains (<<60 μm) still embedded in silicate were not extracted. This fraction amounted to a negligible

mass (<1 mg) and even at very high concentrations of Ru and Mo would have contributed a minor fraction of the analytes. For most samples, the metal grains ranged in size, with most between the 250- and 60- μm sieve mesh sizes, although some grains larger than 250 μm and smaller than 60 μm were present in all samples. The grains from the Apollo 16 samples had bright metallic luster and minimal rust. Metal from the two meteorite samples was more rusted, so fractions that were less magnetic relative to those used for the Apollo samples were processed for NWA 11228. As plenty of relatively silicate-free metal was separated from NWA 5000, only this fraction was processed. The terrestrial weathering of the two meteorites is expected to have no effect on the Ru or Mo isotopic compositions as, compared to the metal, the concentrations of Ru and Mo in the crust are generally low and the isotopic compositions are corrected for any natural (and instrumental) mass fractionation that may have occurred.

Chemical purification procedures

Separated metals were digested either in quartz tubes using 5 ml of concentrated HNO_3 and 2.5 ml of concentrated HCl (*aqua regia*) in an Anton Paar High-Pressure Asher (320°C for 12 hours) (samples NWA 11228 and 60315) or by table-top digestion, using 6 M HCl with traces of HNO_3 (130°C, 48 hours) (samples NWA 5000, 62235, and 68815). The Ru was separated from the matrix and purified using a four-stage cation and anion chromatography procedure similar to that described in (78). Briefly, the samples were slowly dried and converted to 0.2 M HCl , which was loaded onto a pre-cleaned Bio-Rad Econo-Column containing 10 ml of cation resin, from which the Ru and other HSE were eluted with 0.2 M HCl . Molybdenum was eluted in 1 M hydrofluoric acid (HCl)–0.1 M HF . The Ru cuts were dried and then taken up in a 0.2 M HCl –10% Br_2 solution, allowed to rest on a hot plate at 100°C overnight, and loaded onto a ~0.25-ml weak anion DEAE resin column to separate Ru and Pd. The Ru was eluted with 5 ml of 0.2 M HCl –10% Br_2 . The samples were further purified with respect to Zr and Mo by loading and eluting Ru in 1 M HF on a 2-ml anion resin Bio-Rad column. Remaining Zr was eluted in 6 M HCl –1 M HF . For samples with substantial amounts of remaining Mo after the first cation column, Mo was collected in 3 M HNO_3 and combined with the previous Mo cut. Often, not all the Ru was eluted in 1 M HF and was eluted along with Zr in 6 M HCl –1 M HF , and the anion column had to be repeated for this cut. Last, a small version of the cation column described above with 2 ml of cation resin was used to remove the remaining Fe from the Ru, and the anion column was repeated a third or fourth time to remove the remaining Mo. The chemical separation procedures resulted in Mo/Ru between 2×10^{-5} and 4×10^{-4} and Ru/Pd between 4×10^{-6} and 1×10^{-3} , which were sufficiently low for precise and accurate interference corrections to be made (fig. S1) (40). The total analytical blank was <100 pg ($n = 3$), which was negligible for all samples. While concentrations for metals within these rocks are not well constrained due to their wide variability, the yield for the entire separation procedure was ~55 to 90% based on initial contents measured using a Thermo Scientific X-Series quadrupole inductively coupled plasma mass spectrometer (ICP-MS).

The Mo chromatographic procedure was similar to that of (79). Molybdenum cuts from the Ru chemistry were purified of Fe and other matrix elements using a Bio-Rad column filled with 2 ml of anion resin. The samples were loaded, and Fe was eluted in 1 M HF , high-field strength elements were eluted in 6 M HCl –0.01 M HF , W

was eluted in 6 M HCl –1 M HF , and Mo was finally eluted in 3 M HNO_3 . The Mo was further purified of Ru and Zr using a bulb pipette column filled with 1 ml of TRU-Spec resin. This column was done twice: first, loading in 1 M HCl and eluting Mo in 0.1 M HCl , and second, loading in 7 M HNO_3 and eluting Mo in 0.1 M HNO_3 . After this chemistry, Zr/Mo and Ru/Mo were typically between 7×10^{-5} and 3×10^{-4} and between 1×10^{-6} and 3×10^{-5} , respectively. For 60315 during one analysis, the Zr/Mo was somewhat higher ($\sim 9 \times 10^{-4}$), but after repeating the TRU-Spec column, the Zr was 7×10^{-5} , and the two analyses were consistent with one another and with the other lunar impactites. Overall, the Zr/Mo of the purified Mo cuts was low enough for accurate and precise interference corrections (fig. S1) (43). The total analytical blank for Mo was 6 ng ($n = 3$), which was negligible for all samples. The yield for this separation procedure was ~65 to 90%.

Mass spectrometry

Ruthenium and Mo analyses were conducted using a Thermo Scientific Neptune Plus Multicollector MC-ICP-MS at the Institut für Planetologie, University of Münster. Only 70 to 200 ng of Ru and 80 to 200 ng of Mo were extracted from the samples, which reflects the overall low amount of impactor-derived metal in lunar impactites. These quantities of Ru and Mo were insufficient for analyses using previously reported Ru and Mo isotope measurement techniques using 100 parts per billion (ppb) solutions and a standard cone setup for the plasma interface (40, 43). Therefore, an X-skimmer cone was used in place of the standard H-skimmer cone, coupled with a standard sampler cone. This configuration increases the sensitivity by a factor of 2, so 50 ppb solutions could be used for signals of 1 V or greater on ^{100}Ru and 3 V or greater on ^{98}Mo over 100 cycles with 8-s integration times (i.e., the typical setup used in previous studies). To test the accuracy and precision of the measurements with the new cone configuration, several previously measured samples were remeasured, some of which were analyzed in the same sessions as the lunar impactites. These results are summarized in tables S5 and S6 and collectively show that results for all samples were in excellent agreement with previous measurements. Only the Ru isotope analyses for metal separated from Ochansk (H4) gave a slightly lower $\epsilon^{100}\text{Ru}$ using the X-skimmer setup compared to a previous measurement on a bulk sample (40). This difference may reflect using different samples of this meteorite (e.g., variable CRE shielding conditions or using separated metal, instead of bulk powder in a partially equilibrated H4 chondrite); nevertheless, the measured values agree within uncertainty.

The Ru and Mo isotopic compositions are reported in ϵ notation (parts-per- 10^4 deviations from terrestrial standards) and are normalized to $^{99}\text{Ru}/^{101}\text{Ru} = 0.745075$ (80) and $^{98}\text{Mo}/^{96}\text{Mo} = 1.453173$ (81). Interference corrections for $\epsilon^{100}\text{Ru}$ were typically <0.5 ϵ , but for two samples were larger, between 2.7 ϵ (NWA 11228) and 3.4 ϵ (60315). Despite the variable interference corrections, all samples display indistinguishable $\epsilon^{100}\text{Ru}$. This and the fact that the magnitude of the interference corrections is well within the range where accurate corrections can be made (fig. S1) demonstrate the accuracy of these corrections. For $\epsilon^{94}\text{Mo}$ and $\epsilon^{95}\text{Mo}$, the interference corrections were typically 1.3 to 4.7 ϵ and 0.2 to 0.5 ϵ , respectively, which was also within the range of accurate corrections (fig. S1) (43). As for Ru, despite the variable corrections, all impactites have indistinguishable Mo isotope compositions, again demonstrating that these corrections are precise and accurate. This was also monitored by measuring an

ocean island basalt with Zr/Mo between 2×10^{-4} and 4×10^{-4} , which reproduced well with other terrestrial rock data (table S6).

Data for $\epsilon^{96}\text{Ru}$, $\epsilon^{104}\text{Ru}$, $\epsilon^{92}\text{Mo}$, $\epsilon^{97}\text{Mo}$, and $\epsilon^{100}\text{Mo}$ are reported in tables S2 and S3, along with the data presented in the main text for completeness. The $\epsilon^{96}\text{Ru}$ data, however, could not be corrected for Zr interferences, because the cup setup did not allow for monitoring Zr masses. Therefore, the reported $\epsilon^{96}\text{Ru}$ should be considered an upper limit. The $\epsilon^{98}\text{Ru}$ data are not reported, as the low abundance of ^{98}Ru (and of Ru in these samples) limits the precision and accuracy of the ^{98}Ru data. Note that the $\epsilon^{96}\text{Ru}$ and $\epsilon^{104}\text{Ru}$ data are consistent with the measured $\epsilon^{100}\text{Ru}$ and $\epsilon^{102}\text{Ru}$ values, because at $\epsilon^{100}\text{Ru} \sim 0$, the $\epsilon^{96}\text{Ru}$ and $\epsilon^{104}\text{Ru}$ are also expected to be within uncertainty of zero (40), which is observed. Likewise, the $\epsilon^{92}\text{Mo}$, $\epsilon^{97}\text{Mo}$, and $\epsilon^{100}\text{Mo}$ data are also consistent with the $\epsilon^{94}\text{Mo}$ and $\epsilon^{95}\text{Mo}$ data, given that they are all consistent with a similar s-process deficit. Moreover, plots of $\epsilon^{92}\text{Mo}$ or $\epsilon^{94}\text{Mo}$ versus $\epsilon^{95}\text{Mo}$, $\epsilon^{97}\text{Mo}$, or $\epsilon^{100}\text{Mo}$ all show the NC-CC dichotomy, albeit not as definitively as the $\epsilon^{94}\text{Mo}$ versus $\epsilon^{95}\text{Mo}$ plot, and on all these plots, the mean of the lunar impactites falls on the NC array.

Calculation of maximum CC contribution to late accretion

Following (66), the mass fraction of CC material in the impactor population represented by the impactites can be calculated from their position between the NC- and CC-lines in the $\epsilon^{95}\text{Mo}$ - $\epsilon^{94}\text{Mo}$ diagram as $f_{\text{CC}} = (\Delta^{95}\text{Mo}_{\text{Impactites}} - \Delta^{95}\text{Mo}_{\text{NC}}) / (\Delta^{95}\text{Mo}_{\text{CC}} - \Delta^{95}\text{Mo}_{\text{NC}})$, where $\Delta^{95}\text{Mo}$ is defined in Table 1. Using $\Delta^{95}\text{Mo}_{\text{NC}} = -9 \pm 2$, $\Delta^{95}\text{Mo}_{\text{CC}} = +26 \pm 2$ (66), and the $\Delta^{95}\text{Mo}$ of the weighted average of the lunar impactites, we calculate a CC fraction of -0.03 ± 0.26 . However, recent work has shown that the slope of the NC-line is slightly shallower than that of the CC-line, meaning that there is not a single characteristic $\Delta^{95}\text{Mo}$ value for all NC meteorites, which instead depends on the position of a given sample along the NC-line (82). Nevertheless, these nonuniform $\Delta^{95}\text{Mo}$ values among NC meteorites have only a small effect on the overall uncertainty of the calculated CC mass fractions. For instance, given that the lunar impactites plot on the NC-line close to the composition of enstatite chondrites, the NC component in the impactites must have an enstatite chondrite-like Mo isotopic composition. Using the typical $\Delta^{95}\text{Mo} = -7 \pm 4$ of enstatite chondrites in the above equation results in a CC fraction of -0.09 ± 0.29 instead of -0.03 ± 0.26 as calculated using the nominal $\Delta^{95}\text{Mo} = -9 \pm 2$ of the NC reservoir. These two values are essentially identical and indicate that if the impactites are representative of late accretion in general, this would allow only up to ~20 to 25% of CC material in the late accretionary assemblage. We stress, however, that because of the low probability that the true fraction of CC material is at the limit of the uncertainty of the lunar impactite average and considering the BSE-like Ru isotopic composition of the impactors, it is likely that the CC contribution to late accretion would be considerably less than 20 to 25%, and the true CC contribution to late accretion may be much lower (and in fact may be zero).

Statistical analysis

The external reproducibility (2SD) of the Ru and Mo isotope measurements was estimated by repeated analyses of an iron meteorite sample using the same setup as for the lunar impactites, which gave the following results: $\pm 0.49 \epsilon^{96}\text{Ru}$, $\pm 0.14 \epsilon^{100}\text{Ru}$, $\pm 0.17 \epsilon^{102}\text{Ru}$, and $\pm 0.33 \epsilon^{104}\text{Ru}$ ($n = 38$); and $\pm 0.33 \epsilon^{92}\text{Mo}$, $\pm 0.18 \epsilon^{94}\text{Mo}$, $\pm 0.16 \epsilon^{95}\text{Mo}$, $\pm 0.09 \epsilon^{97}\text{Mo}$, and $\pm 0.23 \epsilon^{100}\text{Mo}$ ($n = 17$). This external reproducibility was applied as the uncertainty for samples measured up to three

times. For samples measured more than three times, the 95% CI of the mean was used as the uncertainty. Weighted means were calculated using ISOPLOT (83) and were weighted only by the uncertainty of individual data points. The uncertainty of the weighted mean is the 95% confidence limit, which equals $t\sqrt{\text{MSWD}}$ (mean square weighted deviation). Uncertainties of literature data are the same as reported in those references.

SUPPLEMENTARY MATERIALS

Supplementary material for this article is available at <https://science.org/doi/10.1126/sciadv.abh2837>

REFERENCES AND NOTES

- C.-L. Chou, Fractionation of siderophile elements in the Earth's upper mantle. in *Proc. Lunar. Sci. Conf. 9th*, 219–230 (1978).
- R. J. Walker, Highly siderophile elements in the Earth, Moon and Mars: Update and implications for planetary accretion and differentiation. *Geochemistry* **69**, 101–125 (2009).
- F. Albarède, Volatile accretion history of the terrestrial planets and dynamic implications. *Nature* **461**, 1227–1233 (2009).
- Z. Wang, H. Becker, Ratios of S, Se and Te in the silicate Earth require a volatile-rich late veneer. *Nature* **499**, 328–331 (2013).
- L. Piani, Y. Marrocchi, T. Rigaudier, L. G. Vacher, D. Thomassin, B. Marty, Earth's water may have been inherited from material similar to enstatite chondrite meteorites. *Science* **369**, 1110–1113 (2020).
- B. Marty, The origins and concentrations of water, carbon, nitrogen and noble gases on Earth. *Earth Planet. Sci. Lett.* **313**, 56–66 (2012).
- M. Fischer-Gödde, B.-M. Elfers, C. Münker, K. Szilas, W. D. Maier, N. Messling, T. Morishita, M. Van Kranendonk, H. Smithies, Ruthenium isotope vestige of Earth's pre-late-veener mantle preserved in Archaean rocks. *Nature* **579**, 240–244 (2020).
- M. I. Varas-Reus, S. König, A. Yierpan, J.-P. Lorand, R. Schoenberg, Selenium isotopes as tracers of a late volatile contribution to Earth from the outer Solar System. *Nat. Geosci.* **12**, 779–782 (2019).
- G. W. Wetherill, Late heavy bombardment of the moon and terrestrial planets, in *Lunar Sci. Conf. 6th*, 1539–1561 (1975).
- F. Tera, D. A. Papanastassiou, G. J. Wasserburg, Isotopic evidence for a terminal lunar cataclysm. *Earth Planet. Sci. Lett.* **22**, 1–21 (1974).
- W. F. Bottke, M. D. Norman, The late heavy bombardment. *Annu. Rev. Earth Planet. Sci.* **45**, 619–647 (2017).
- G. Neukum, B. A. Ivanov, W. K. Hartmann, Cratering records in the inner solar system in relation to the lunar reference system. *Space Sci. Rev.* **96**, 55–86 (2001).
- G. A. Schaeffer, O. A. Schaeffer, $^{39}\text{Ar}/^{40}\text{Ar}$ ages of lunar rocks, in *Proc. Lunar Sci. Conf. 8th*, 2253–2300 (1977).
- L. A. Haskin, R. L. Korotev, K. M. Rockow, B. L. Jolliff, The case for an Imbrium origin of the Apollo thorium-rich impact-melt breccias. *Meteorit. Planet. Sci.* **33**, 959–975 (1998).
- V. A. Fernandes, J. Fritz, B. P. Weiss, I. Garrick-Bethell, D. L. Shuster, The bombardment history of the Moon as recorded by ^{40}Ar - ^{39}Ar chronology. *Meteorit. Planet. Sci.* **48**, 241–269 (2013).
- M. D. Norman, A. A. Nemchin, A 4.2 billion year old impact basin on the Moon: U-Pb dating of zirconolite and apatite in lunar melt rock 67955. *Earth Planet. Sci. Lett.* **388**, 387–398 (2014).
- L. F. White, A. Černok, J. R. Darling, M. J. Whitehouse, K. H. Joy, C. Cayron, J. Dunlop, K. T. Tait, M. Anand, Evidence of extensive lunar crust formation in impact melt sheets 4,330 Myr ago. *Nat. Astron.* **4**, 974–978 (2020).
- B. A. Cohen, T. D. Swindle, D. A. Kring, Geochemistry and 40Ar-39Ar geochronology of impact-melt clasts in feldspathic lunar meteorites: Implications for lunar bombardment history. *Meteorit. Planet. Sci.* **40(5)**, 755–777 (2005).
- B. A. Cohen, The Vestan cataclysm: Impact-melt clasts in howardites and the bombardment history of 4 Vesta. *Meteorit. Planet. Sci.* **48**, 771–785 (2013).
- S. Marchi, W. F. Bottke, B. A. Cohen, K. Wünnemann, D. A. Kring, H. Y. McSween, M. C. De Sanctis, D. P. O'Brien, P. Schenk, C. A. Raymond, C. T. Russell, High-velocity collisions from the lunar cataclysm recorded in asteroidal meteorites. *Nat. Geosci.* **6**, 303–307 (2013).
- D. A. Kring, B. A. Cohen, Cataclysmic bombardment throughout the inner solar system 3.9–4.0 Ga. *J. Geophys. Res. E Planets* **107**, 5009 (2002).
- N. E. B. Zellner, Cataclysm no more: New views on the timing and delivery of lunar impactors. *Orig. Life Evol. Biosph.* **47**, 261–280 (2017).
- W. K. Hartmann, History of the terminal cataclysm paradigm: Epistemology of a planetary bombardment that never (?) happened. *Geosciences* **9**, 285 (2019).

24. R. Gomes, H. F. Levison, K. Tsiganis, A. Morbidelli, Origin of the cataclysmic Late Heavy Bombardment period of the terrestrial planets. *Nature* **435**, 466–469 (2005).
25. K. Tsiganis, R. Gomes, A. Morbidelli, H. F. Levison, Origin of the orbital architecture of the giant planets of the Solar System. *Nature* **435**, 459–461 (2005).
26. M. Clement, N. A. Kaib, S. N. Raymond, K. J. Walsh, Mars' growth stunted by an early giant planet instability. *Icarus* **311**, 340–356 (2018).
27. M. S. Clement, N. A. Kaib, S. N. Raymond, J. E. Chambers, K. J. Walsh, The early instability scenario: Terrestrial planet formation during the giant planet instability, and the effect of collisional fragmentation. *Icarus* **321**, 778–790 (2019).
28. S. J. Mojzsis, R. Brasser, N. M. Kelly, O. Abramov, S. C. Werner, Onset of giant planet migration before 4480 million years ago. *Astrophys. J.* **881**, 44 (2019).
29. R. R. de Sousa, A. Morbidelli, S. N. Raymond, A. Izidoro, R. Gomes, E. Vieira Neto, Dynamical evidence for an early giant planet instability. *Icarus* **339**, 113605 (2020).
30. D. Nesvorný, F. V. Roig, R. Deienno, The role of early giant-planet instability in terrestrial planet formation. *Astron. J.* **161**, 50 (2021).
31. M. D. Norman, V. C. Bennett, G. Ryder, Targeting the impactors: Siderophile element signatures of lunar impact melts from Serenitatis. *Earth Planet. Sci. Lett.* **202**, 217–228 (2002).
32. I. S. Puchtel, R. J. Walker, O. B. James, D. A. Kring, Osmium isotope and highly siderophile element systematics of lunar impact melt breccias: Implications for the late accretion history of the Moon and Earth. *Geochim. Cosmochim. Acta* **72**, 3022–3042 (2008).
33. M. Fischer-Gödde, H. Becker, Osmium isotope and highly siderophile element constraints on ages and nature of meteoritic components in ancient lunar impact rocks. *Geochim. Cosmochim. Acta* **77**, 135–156 (2012).
34. J. Liu, M. Sharp, R. D. Ash, D. A. Kring, R. J. Walker, Diverse impactors in Apollo 15 and 16 impact melt rocks: Evidence from osmium isotopes and highly siderophile elements. *Geochim. Cosmochim. Acta* **155**, 122–153 (2015).
35. P. Gleißner, H. Becker, Formation of Apollo 16 impactites and the composition of late accreted material: Constraints from Os isotopes, highly siderophile elements and sulfur abundances. *Geochim. Cosmochim. Acta* **200**, 1–24 (2017).
36. E. C. McIntosh, J. M. D. Day, Y. Liu, C. Jiskoot, Examining the compositions of impactors striking the Moon using Apollo impact melt coats and anorthositic regolith breccia meteorites. *Geochim. Cosmochim. Acta* **274**, 192–210 (2020).
37. H. Becker, M. F. Horan, R. J. Walker, S. Gao, J. P. Lorand, R. L. Rudnick, Highly siderophile element composition of the Earth's primitive upper mantle: Constraints from new data on peridotite massifs and xenoliths. *Geochim. Cosmochim. Acta* **70**, 4528–4550 (2006).
38. M. Fischer-Gödde, T. Kleine, Ruthenium isotopic evidence for an inner Solar System origin of the late veneer. *Nature* **541**, 525–527 (2017).
39. E. A. Worsham, C. Burkhardt, G. Budde, M. Fischer-Gödde, T. S. Kruijjer, T. Kleine, Distinct evolution of the carbonaceous and non-carbonaceous reservoirs: Insights from Ru, Mo, and W isotopes. *Earth Planet. Sci. Lett.* **521**, 103–112 (2019).
40. M. Fischer-Gödde, C. Burkhardt, T. S. Kruijjer, T. Kleine, Ru isotope heterogeneity in the solar protoplanetary disk. *Geochim. Cosmochim. Acta* **168**, 151–171 (2015).
41. T. Hopp, G. Budde, T. Kleine, Heterogeneous accretion of Earth inferred from Mo-Ru isotope systematics. *Earth Planet. Sci. Lett.* **534**, 116065 (2020).
42. N. Dauphas, B. Marty, L. Reisberg, Molybdenum evidence for inherited planetary scale isotope heterogeneity of the protosolar nebula. *Astrophys. J.* **565**, 640–644 (2002).
43. G. Budde, C. Burkhardt, G. A. Brennecka, M. Fischer-Gödde, T. S. Kruijjer, T. Kleine, Molybdenum isotopic evidence for the origin of chondrules and a distinct genetic heritage of carbonaceous and non-carbonaceous meteorites. *Earth Planet. Sci. Lett.* **454**, 293–303 (2016).
44. T. S. Kruijjer, C. Burkhardt, G. Budde, T. Kleine, Age of Jupiter inferred from the distinct genetics and formation times of meteorites. *Proc. Natl. Acad. Sci. U.S.A.* **114**, 6712–6716 (2017).
45. P. H. Warren, Stable-isotopic anomalies and the accretionary assemblage of the Earth and Mars: A subordinate role for carbonaceous chondrites. *Earth Planet. Sci. Lett.* **311**, 93–100 (2011).
46. M. D. Norman, R. A. Duncan, J. J. Huard, Identifying impact events within the lunar cataclysm from ^{40}Ar - ^{39}Ar ages and compositions of Apollo 16 impact melt rocks. *Geochim. Cosmochim. Acta* **70**, 6032–6049 (2006).
47. M. L. Grange, M. D. Norman, V. C. Bennett, A possible 4.1–4.2 Ga impact event recorded in lunar meteorite Northwest Africa 5000, in *79th Annual Meeting of the Meteoritical Society*, 6300 (2016).
48. T. Liu, G. Michael, K. Wünnemann, H. Becker, J. Oberst, Lunar megaregolith mixing by impacts: Spatial diffusion of basin melt and its implications for sample interpretation. *Icarus* **339**, 113609 (2020).
49. R. J. Walker, K. Bermingham, J. Liu, I. S. Puchtel, M. Touboul, E. A. Worsham, In search of late-stage planetary building blocks. *Chem. Geol.* **411**, 125–142 (2015).
50. N. Dauphas, The isotopic nature of the Earth's accreting material through time. *Nature* **541**, 521–524 (2017).
51. R. L. Korotev, Compositional variation in Apollo 16 impact-melt breccias and inferences for the geology and bombardment history of the Central Highlands of the Moon. *Geochim. Cosmochim. Acta* **58**, 3931–3969 (1994).
52. H. Wänke, H. Palme, H. Baddenhausen, G. Dreibus, E. Jagoutz, H. Kruse, B. Spettel, F. Teschke, R. Thacker, Chemistry of Apollo 16 and 17 samples: Bulk composition, late stage accumulation and early differentiation of the Moon, in *Proc. Lunar Sci. Conf. 5th*, 1307–1335 (1974).
53. P. D. Spudis, Apollo 16 site geology and impact melts: Implications for the geologic history of the lunar highlands. *J. Geophys. Res. Solid Earth* **89**, C95–C107 (1984).
54. A. J. Irving, S. M. Kuehner, R. L. Korotev, D. Rumble III, C. Hupé, Petrology and bulk composition of large lunar feldspathic leucogabbroic breccia Northwest Africa 5000, in *Lunar and Planetary Science Conference 39* (2008).
55. A. Ruzicka, J. Grossman, A. Bouvier, C. B. Agee, The Meteoritical Bulletin, No. 103. *Meteorit. Planet. Sci.* **52**, 1014 (2017).
56. A. Bouvier, J. Gattacceca, C. Agee, J. Grossman, K. Metzler, The Meteoritical Bulletin, No. 104. *Meteorit. Planet. Sci.* **52**, 2284 (2017).
57. J. Gattacceca, A. Bouvier, J. Grossman, K. Metzler, M. Uehara, The Meteoritical Bulletin, No. 106. *Meteorit. Planet. Sci.* **54**, 469–471 (2019).
58. G. Ryder, P. Spudis, Chemical composition and origin of Apollo 15 impact melts. *J. Geophys. Res.* **92**, E432–E446 (1987).
59. T. D. Swindle, P. D. Spudis, G. J. Taylor, R. L. Korotev, R. G. Nichols Jr., C. T. Olinger, Searching for Crisium basin ejecta: Chemistry and ages of Luna 20 impact melts, in *Proc. Lunar Planet. Sci.* (1991).
60. P. Gleißner, H. Becker, New constraints on the formation of lunar mafic impact melt breccias from S-Se-Te and highly siderophile elements. *Meteorit. Planet. Sci.* **55**, 2044–2065 (2020).
61. M. Touboul, I. S. Puchtel, R. J. Walker, Tungsten isotopic evidence for disproportional late accretion to the Earth and Moon. *Nature* **520**, 530–533 (2015).
62. M. Humayun, A. J. Irving, Impactor metal in gabbroic lunar meteorite Northwest Africa 5000, in *18th Annual Goldschmidt Conference* (2008).
63. W. F. Bottke, D. Vokrouhlický, D. Minton, D. Nesvorný, A. Morbidelli, R. Brasser, B. Simonson, H. F. Levison, An Archaean heavy bombardment from a destabilized extension of the asteroid belt. *Nature* **485**, 78–81 (2012).
64. A. Morbidelli, S. Marchi, W. F. Bottke, D. A. Kring, A sawtooth-like timeline for the first billion years of lunar bombardment. *Earth Planet. Sci. Lett.* **355–356**, 144–151 (2012).
65. A. Morbidelli, D. Nesvorný, V. Laurenz, S. Marchi, D. C. Rubie, L. Elkins-Tanton, M. Wiczcerek, S. Jacobson, The timeline of the lunar bombardment: Revisited. *Icarus* **305**, 262–276 (2018).
66. G. Budde, C. Burkhardt, T. Kleine, Molybdenum isotopic evidence for the late accretion of outer Solar System material to Earth. *Nat. Astron.* **3**, 736–741 (2019).
67. S. König, J. P. Lorand, A. Luguet, D. Graham Pearson, A non-primitive origin of near-chondritic S-Se-Te ratios in mantle peridotites; implications for the Earth's late accretionary history. *Earth Planet. Sci. Lett.* **385**, 110–121 (2014).
68. J. L. Hellmann, T. Hopp, C. Burkhardt, H. Becker, M. Fischer-Gödde, T. Kleine, Tellurium isotope geochemistry: Implications for volatile fractionation in chondrite parent bodies and origin of the late veneer. *Geochim. Cosmochim. Acta* **309**, 313–328 (2021).
69. G. Ryder, M. D. Norman, *Catalog of Apollo 16 rocks* (NASA Johnson Space Center, Houston, 1980).
70. R. L. Korotev, Lunar meteorite: Northwest Africa 8673 clan, *Dep. Earth Planet. Sci. Washing. Univ. St. Louis* (2020); https://sites.wustl.edu/meteoritesite/items/lm_nwa_08673_clan/.
71. R. J. Drozd, C. M. Hohenberg, C. J. Morgan, C. E. Ralston, Cosmic-ray exposure history at the Apollo 16 and other lunar sites: Lunar surface dynamics. *Geochim. Cosmochim. Acta* **38**, 1625–1642 (1974).
72. O. A. Schaeffer, L. Husain, G. A. Schaeffer, Ages of highland rocks: The chronology of lunar basin formation revisited, in *Proc. Lunar Sci. Conf. 7th*, 2067–2092 (1976).
73. K. Nishiizumi, M. W. Caffee, N. Vogel, R. Wieler, M. D. Leclerc, A. J. T. Jull, Exposure history of lunar meteorite Northwest Africa 5000, in *40th Lunar and Planetary Science Conference* (2009).
74. J. M. D. Day, R. J. Walker, O. B. James, I. S. Puchtel, Osmium isotope and highly siderophile element systematics of the lunar crust. *Earth Planet. Sci. Lett.* **289**, 595–605 (2010).
75. M. D. Norman, L. E. Borg, L. E. Nyquist, D. D. Bogard, Chronology, geochemistry, and petrology of a ferroan noritic anorthositic clast from Descartes breccia 67215: Clues to the age, origin, structure, and impact history of the lunar crust. *Meteorit. Planet. Sci.* **38**, 645–661 (2003).
76. K. C. Misra, L. A. Taylor, Characteristics of metal particles in Apollo 16 rocks, in *Proc. Lunar Sci. Conf. 6th*, 615–639 (1975).
77. G. W. Pearce, G. S. Hoye, D. W. Strangway, B. M. Walker, L. A. Taylor, Some complexities in the determination of lunar paleointensities, in *Proc. Lunar Sci. Conf. 7th*, 3271–3297 (1976).
78. T. Hopp, T. Kleine, Nature of late accretion to Earth inferred from mass-dependent Ru isotopic compositions of chondrites and mantle peridotites. *Earth Planet. Sci. Lett.* **494**, 50–59 (2018).
79. C. Burkhardt, T. Kleine, F. Oberli, A. Pack, B. Bourdon, R. Wieler, Molybdenum isotope anomalies in meteorites: Constraints on solar nebula evolution and origin of the Earth. *Earth Planet. Sci. Lett.* **312**, 390–400 (2011).

80. J. H. Chen, D. A. Papanastassiou, G. J. Wasserburg, Ruthenium endemic isotope effects in chondrites and differentiated meteorites. *Geochim. Cosmochim. Acta* **74**, 3851–3862 (2010).
81. Q. Lu, A. Masuda, The isotopic composition and atomic weight of molybdenum. *Int. J. Mass Spectrom. Ion Process.* **130**, 65–72 (1994).
82. F. Spitzer, C. Burkhardt, G. Budde, T. Kruijjer, A. Morbidelli, T. Kleine, Isotopic evolution of the inner solar system inferred from molybdenum isotopes in meteorites. *Astrophys. J.* **898**, 1 (2020).
83. K. R. Ludwig, User's manual for Isoplot 3.00, a geochronological toolkit for Microsoft Excel. Berkeley Geochronology Center special publication no.4. *Components* (2003).
84. M. R. Savina, A. M. Davis, C. E. Tripa, M. J. Pellin, R. Gallino, R. S. Lewis, S. Amari, extinct technetium in silicon carbide stardust grains: Implications for stellar nucleosynthesis. *Science* **303**, 649–652 (2004).
85. J. C. Lail, D. W. Hill, R. A. Schmitt, Chemical studies of Apollo 16 and 17 samples, in *Proc. Lunar Sci. Conf. 5th*, 1047–1056 (1974).
86. A. B. Nagurney, A. H. Treiman, P. D. Spudis, Petrology, bulk composition, and provenance of meteorite Northwest Africa 5000 (NWA 5000), in *Lunar and Planetary Science Conference 47* (2016).
87. K. R. Bermingham, E. A. Worsham, R. J. Walker, New insights into Mo and Ru isotope variation in the nebula and terrestrial planet accretionary genetics. *Earth Planet. Sci. Lett.* **487**, 221–229 (2018).
88. C. D. Hilton, K. R. Bermingham, R. J. Walker, T. J. McCoy, Genetics, crystallization sequence, and age of the South Byron Trio iron meteorites: New insights to carbonaceous chondrite (CC) type parent bodies. *Geochim. Cosmochim. Acta* **251**, 217–228 (2019).
89. J. Render, M. Fischer-Gödde, C. Burkhardt, T. Kleine, The cosmic molybdenum-neodymium isotope correlation and the building material of the Earth. *Geochemical Perspect. Lett.* **3**, 170–178 (2017).
90. E. A. Worsham, K. R. Bermingham, R. J. Walker, Characterizing cosmochemical materials with genetic affinities to the Earth: Genetic and chronological diversity within the IAB iron meteorite complex. *Earth Planet. Sci. Lett.* **467**, 157–166 (2017).
91. C. Burkhardt, N. Dauphas, H. Tang, M. Fischer-Gödde, L. Qin, J. H. Chen, S. S. Rout, A. Pack, P. R. Heck, D. A. Papanastassiou, In search of the Earth-forming reservoir: Mineralogical, chemical, and isotopic characterizations of the ungrouped achondrite NWA 5363/NWA 5400 and selected chondrites. *Meteorit. Planet. Sci.* **52**, 807–826 (2017).
92. T. Yokoyama, Y. Nagai, R. Fukai, T. Hirata, Origin and evolution of distinct molybdenum isotopic variabilities within carbonaceous and noncarbonaceous reservoirs. *Astrophys. J.* **883**, 62 (2019).
93. G. M. Poole, M. Rehkämper, B. J. Coles, T. Goldberg, C. L. Smith, Nucleosynthetic molybdenum isotope anomalies in iron meteorites – new evidence for thermal processing of solar nebula material. *Earth Planet. Sci. Lett.* **473**, 215–226 (2017).
94. C. Burkhardt, R. C. Hin, T. Kleine, B. Bourdon, Evidence for Mo isotope fractionation in the solar nebula and during planetary differentiation. *Earth Planet. Sci. Lett.* **391**, 201–211 (2014).
95. G. Budde, T. S. Kruijjer, T. Kleine, Hf-W chronology of CR chondrites: Implications for the timescales of chondrule formation and the distribution of ^{26}Al in the solar nebula. *Geochim. Cosmochim. Acta* **222**, 284–304 (2018).
96. C. D. Hilton, "Genetics, Ages, and Chemical Compositions of Iron Meteorites," dissertation, University of Maryland, College Park, MD (2020).

Acknowledgments: We thank CAPTEM, NASA, and R. Zeigler for providing the Apollo lunar samples, K. Metzler for help in purchasing the lunar meteorites, and U. Heitmann for help with sample preparation. We are grateful to K. Hodges for editorial handling and to M. Norman and four other anonymous reviewers for their insightful comments. This is TRR publication no. 150. **Funding:** This study was funded by Deutsche Forschungsgemeinschaft (DFG; German Research Foundation), project ID 263649064–TRR 170. **Author contributions:** E.A.W. and T.K. designed this study. E.A.W. conducted the analytical work, and E.A.W. and T.K. discussed the results and wrote the manuscript. **Competing interests:** The authors declare that they have no competing interests. **Data and materials availability:** All data needed to evaluate the conclusions in the paper are present in the paper and/or the Supplementary Materials.

Submitted 26 February 2021
Accepted 13 September 2021
Published 29 October 2021
10.1126/sciadv.abh2837

Citation: E. A. Worsham, T. Kleine, Late accretionary history of Earth and Moon preserved in lunar impactites. *Sci. Adv.* **7**, eabh2837 (2021).